

Direct growth of carbon nanotube junctions by a two-step chemical vapor deposition

Zhong Jin, Xuemei Li, Weiwei Zhou, Zuoyan Han, Yan Zhang, Yan Li *

Beijing National Laboratory for Molecular Sciences, Key Laboratory for the Physics and Chemistry of Nanodevices, College of Chemistry and Molecular Engineering, Peking University, Beijing 100871, China

Received 24 July 2006; in final form 30 August 2006
Available online 14 October 2006

Abstract

A simple two-step chemical vapor deposition (CVD) strategy was designed for the direct growth of all-carbon nanojunctions constituted by jointed carbon nanotubes. In the process, Fe–Mo nanoparticles were used as the catalysts, while C_2H_2 and CH_4 were used as the feeding gas in the first and second CVD steps, respectively. By changing temperature and switching carbon source gases in the CVD process, various nanojunctions composed of single-walled and multi-walled carbon nanotubes were prepared. These all-carbon nanojunctions are expected to show special mechanical and electrical properties for the potential applications as the field-emission probes, scanning probe microscope tips and field-effect transistors.

© 2006 Elsevier B.V. All rights reserved.

1. Introduction

One-dimensional (1D) nano-scaled junction structures can be fabricated by joining nanowires, nanorods or nanotubes. For example, the fabrication of metal/semiconductor nanowire heterostructures and their application to field emission transistors (FETs) was reported by Lieber et al. [1]. The dissimilar properties of the two parts of the junctions lead to the unique behaviors of the entire nanostructures. Therefore, the controllable preparation of different 1D nanojunctions ought to be significant for construction of prospective nanodevices.

Carbon nanotubes have attracted extensive attention because of their unique properties and potential applications in broad areas of science and technology [2–4]. Especially, considered as ideal 1D quantum wires, carbon nanotubes (CNTs) are competitive candidates for the connective or/and functional components of nano-devices and nanocircuits [4]. Therefore, various nanojunctions with CNTs taking part in are of special interest. Junctions of multi-walled carbon nanotube (MWNT)/silicon nanowire

[5], single-walled carbon nanotube (SWNT)/carbide nanorod [6], and MWNT/metal nanowire [7,8] have already been reported.

Known that CNTs with diverse diameter and helicity can be either metallic or semi-conducting, it is possible to fabricate all-carbon nanojunctions with different morphologies and electronic properties by joining two or more CNT segments. Iijima et al. indicated that CNT junctions could be formed by joining MWNT segments through pentagonal–heptagonal topological defects [9,10]. Then, intermolecular junctions of SWNTs with different diameters, helices or/and connecting angles were predicted and observed [11–15]. But these intratube SWNT junctions were got occasionally. Recently, different intratube MWNT junctions were fabricated [16–22]. MWNT/MWNT junctions were obtained in porous anodic aluminum oxide templates [17], by arc-discharge [18] or two-step plasma-enhanced CVD methods [19]. ^{12}C – ^{13}C MWNT intratube-junction arrays were prepared by a ^{13}C -ethylene isotope labeling method [16]. CN_x -Carbon and BCN-Carbon nanotube junctions were fabricated by introducing different doping gases at the midway of CVD process [20,21]. Rao et al. [22] discovered that Ti-doped Fe catalysts grew Y-junction MWNTs due to the attachment of catalyst par-

* Corresponding author. Fax: +86 10 62756773.
E-mail address: yanli@pku.edu.cn (Y. Li).

ticles on the growing MWNT walls. Nevertheless, the direct growth of SWNT–MWNT intratube junctions has rarely been discussed. And the controllable fabrication of multifarious nanostructures based on CNTs is still challenging.

Here we report a simple two-step catalytic CVD method for the growth of novel ‘injector-like’ or ‘dropper-like’ nanojunctions constituted by different types of CNTs. These junctions may act as building blocks for nanodevices or nanocircuits consisting of only one element [12]. Considering the unique geometric shape, the excellent conductivity and the outstanding mechanical strength, they are also expected to be applied as field emitters, scanning probes and components for field emission transistors.

2. Experimental section

Mono-dispersed Fe–Mo nanoparticles were prepared with a method similar to Ref. [23]. Instead of the expensive dioctyl ether, here we used diphenyl ether as the solvent. Typically, 0.098 g (0.50 mmol) of $\text{Fe}(\text{CO})_5$ and 0.031 g (0.12 mmol) of $\text{Mo}(\text{CO})_6$ were mixed with 0.186 g (0.66 mmol) of oleic acid and 0.270 g (1.0 mmol) of octadecyl amine in 5 ml of diphenyl ether. The solutions were refluxed under nitrogen for 30 min to obtain Fe–Mo nanoparticles. Ethanol was added to precipitate the nanoparticles. The average diameter of the produced nanoparticles was 8.0 nm. The precipitates were re-dispersed in cyclohexane and loaded onto the selected catalyst supports (silica microspheres, Na-ZSM-5 zeolite, porous silica and porous magnesia) by soakage.

The CVD procedures were schemed in Fig. 1a. The catalyst held in a quartz boat was put into the tubular furnace equipped with a quartz tube, heated to 750 °C under 500 sccm of Ar and reduced by 350 sccm of H_2 for 25 min. 100 sccm of C_2H_2 in 300–600 sccm of H_2 was intro-

duced into the system for 6–10 min at 750 °C to grow MWNTs with catalyst nanoparticles remained on the tips (Fig. 1b,c). This is the *ethyne step*. Then the gas flow was switched to 500 sccm Ar, at the same time, the furnace temperature was rapidly increased to 950 °C (Scheme 1) or cooled down to 500 °C in about 5 min then re-heated to 950 °C (Scheme 2). Whereafter Ar flow was switched to 400 sccm of CH_4 together with 0–250 sccm of H_2 for 15 min to grow CNT junctions. This is the *methane step*. Finally, the furnace was cooled down to room temperature under Ar atmosphere.

The products were characterized by a JEM200CX transmission electron microscope (TEM) operated at 120 kV and a Hitachi-9000 high-resolution transmission electron microscope (HRTEM) operated at 100 kV. Raman spectra were measured using a Renishaw 1000 micro-Raman Spectrometer with the 514.5 nm line of an Ar ion laser as the excitation source.

3. Results and discussion

3.1. Dropper-like SWNT/MWNT nanojunctions obtained by Scheme 1

Typical TEM images of the CNT junctions fabricated on silica microspheres by the two-step CVD process without halfway furnace cooling-down (Scheme 1) are shown in Fig. 2a,b. The thick parts of these junctions are MWNTs with average diameter of 20 nm. HRTEM images (Fig. 2c,d) showed that the thin parts are SWNTs with the diameters of 1.3–2.4 nm. The radial breathing mode (RBM) band in the Raman spectrum (Fig. 2e) also indicated the existence of SWNTs. The MWNT parts were gradually shrunk to form a conic cap and the inner layer of MWNTs smoothly joined the SWNT parts. In some cases, the thin parts were made of SWNT bundles. The

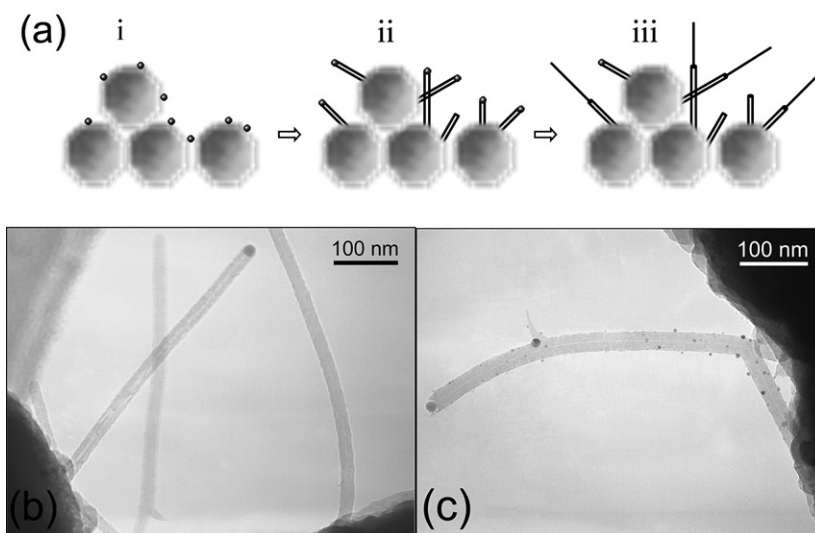


Fig. 1. (a) Schematic show of the two-step CVD process employed to fabricate CNT junctions, (i) Catalyst of Fe–Mo nanoparticles on the silica microspheres, (ii) Fabrication of MWNTs by decomposition of C_2H_2 (ethyne step), (iii) CNTs with smaller diameters grown from the MWNTs by decomposition of CH_4 and formation of CNT junctions (*methane step*). (b, c) TEM images of MWNTs obtained after the first ethyne CVD step.

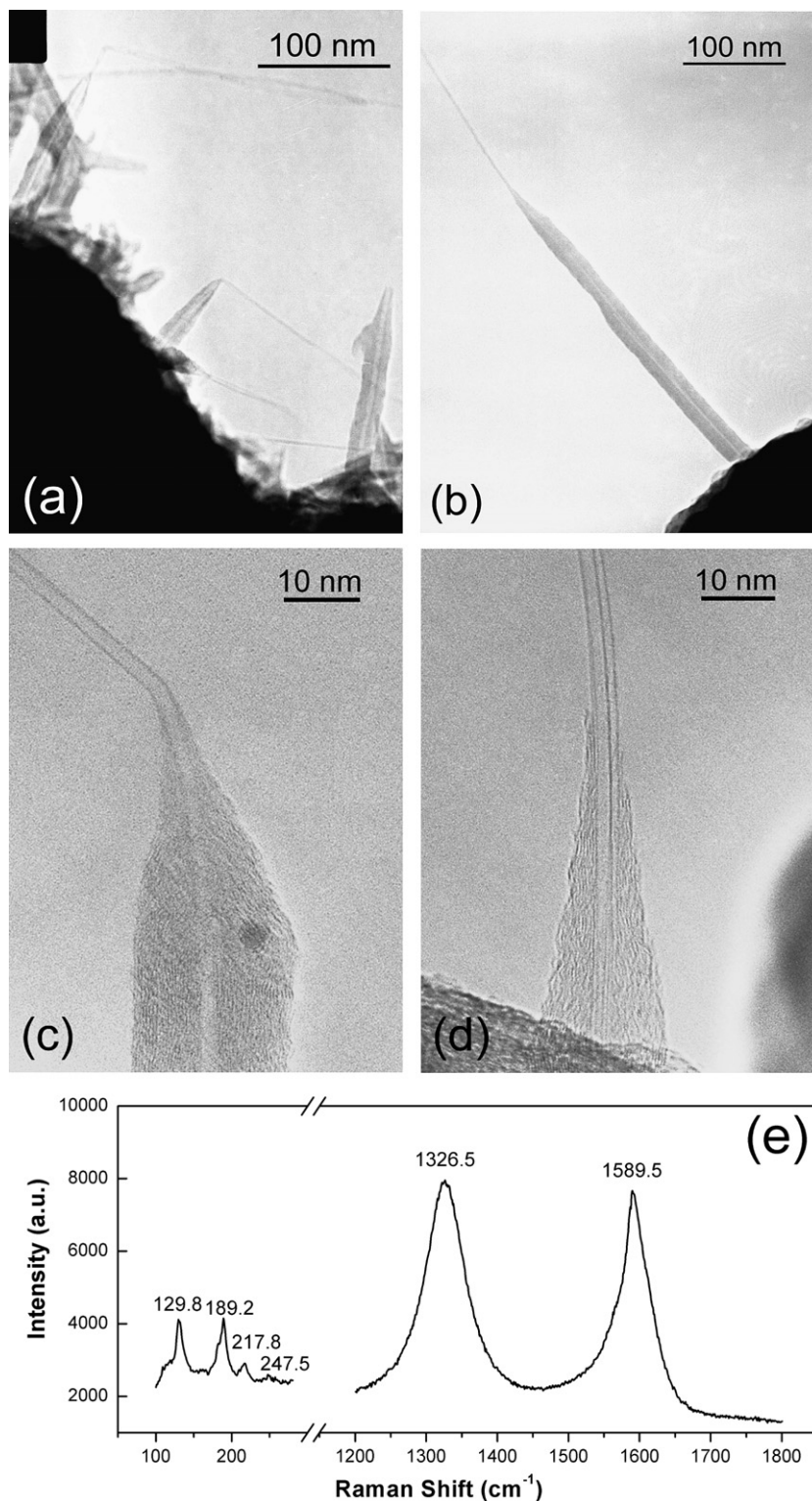


Fig. 2. TEM (a, b) and HRTEM (c, d) images and the Raman spectrum (e) of the dropper-like SWNT/MWNT junctions obtained via Scheme 1 without the cooling-down process between the two CVD steps.

SWNTs in the bundles were either jointed with the inner layers of MWNTs, or grown out from the midsections of the conic MWNT caps. It is noticeable that the inner diameters of the MWNT parts are always similar to those of the SWNT parts. In the products under this CVD condition,

we rarely observed CNT junctions with inner diameter larger than 3 nm, implying that the MWNTs with small inner diameter are beneficial to the growth of SWNT/MWNT junctions. Except CNT junctions and some ordinary MWNTs, we hardly found any isolated SWNTs or

SWNT-bundles in the products. The absence of independent SWNTs in the products may be caused by that almost all of the Fe–Mo nanoparticles had been used to grow MWNTs or passivated by carbon after the *ethyne step*, and there are little active catalyst particles for the growth of individual SWNTs.

For comparison, we terminated the CVD process immediately after the *ethyne step*. It was found that the products are mainly made of MWNTs with average diameters of 20 nm, and some MWNTs have nanoparticles remained on the tips (Fig. 1b,c). Combining with the morphology of the products via Scheme 1, we could deduce that the

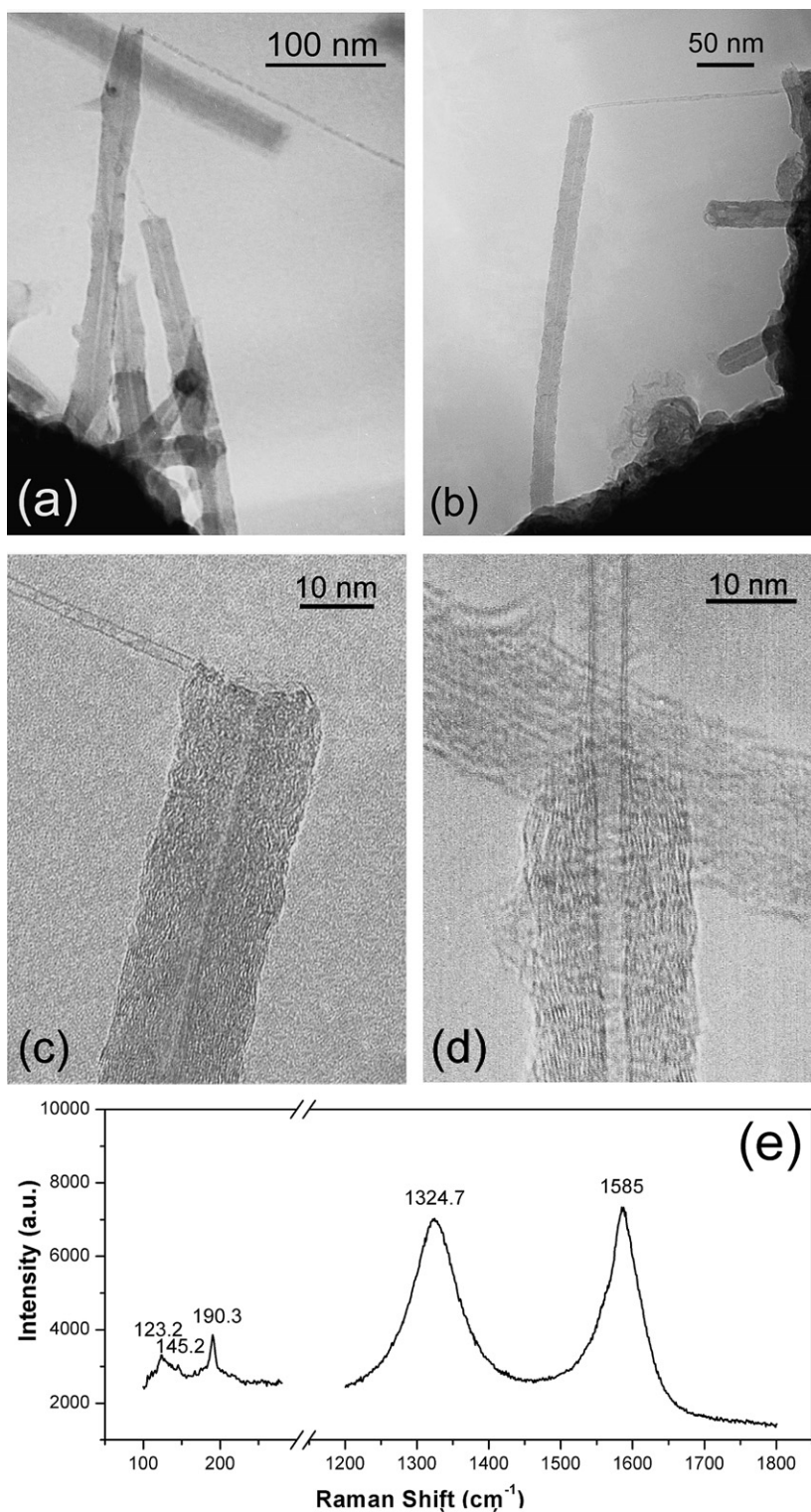


Fig. 3. TEM (a, b) and HRTEM (c, d) images and the Raman spectrum (e) of the injector-like CNT junctions obtained via Scheme 2 with the cooling-down process between the two CVD steps.

MWNTs for the growth of CNT junctions were formed through ‘tip-growth’ mechanism. We will show hereafter that this is also the case for Scheme 2. The nanoparticles remained on the tips of MWNTs acted as catalyst to grow the thin parts of junctions. Through the rapid gas switching and reheating step in Scheme 1, MWNTs gradually shrunk to form conic tips because Ar flow diluted the remained ethyne gas. And the evaporation or splitting into parts reduced the dimensions of the remained catalyst nanoparticles to a proper size for the formation of SWNTs or SWNT-bundles in *methane step*.

3.2. Injector-like SWNT/MWNT and double-walled carbon nanotube (DWNT)/MWNT nanojunctions obtained by Scheme 2

In another experimental scheme, the furnace was cooled down to 500 °C in about 5 min after the ethyne CVD step

and then re-heated to 950 °C, followed by methane CVD step (Scheme 2). With this half-way cooled-down process, we obtained CNT junctions with an injector-like morphology as show in Fig. 3a,b. The thick parts of the junctions are MWNTs and the thin parts are SWNTs or DWNTs with observed tube diameters of 1.5–4.1 nm. The inner layers of the MWNT parts jointed with the SWNT or DWNT parts as shown in the HRTEM images (Fig. 3c,d). The Raman spectrum (Fig. 3e) also gave the circumstantial evidence of the CNT junctions’ existence. Similar to the products through Scheme 1, the MWNT parts of CNT junctions also have inner diameters similar to those of the SWNT or DWNT parts. Also, we never found any independent SWNTs or SWNT-bundles in the products.

While in Scheme 2, the furnace was suddenly cooled down after *ethyne step*, so that the growth of MWNTs was interrupted and led to the formation of open ends. The remained nanoparticles catalyzed the growth of

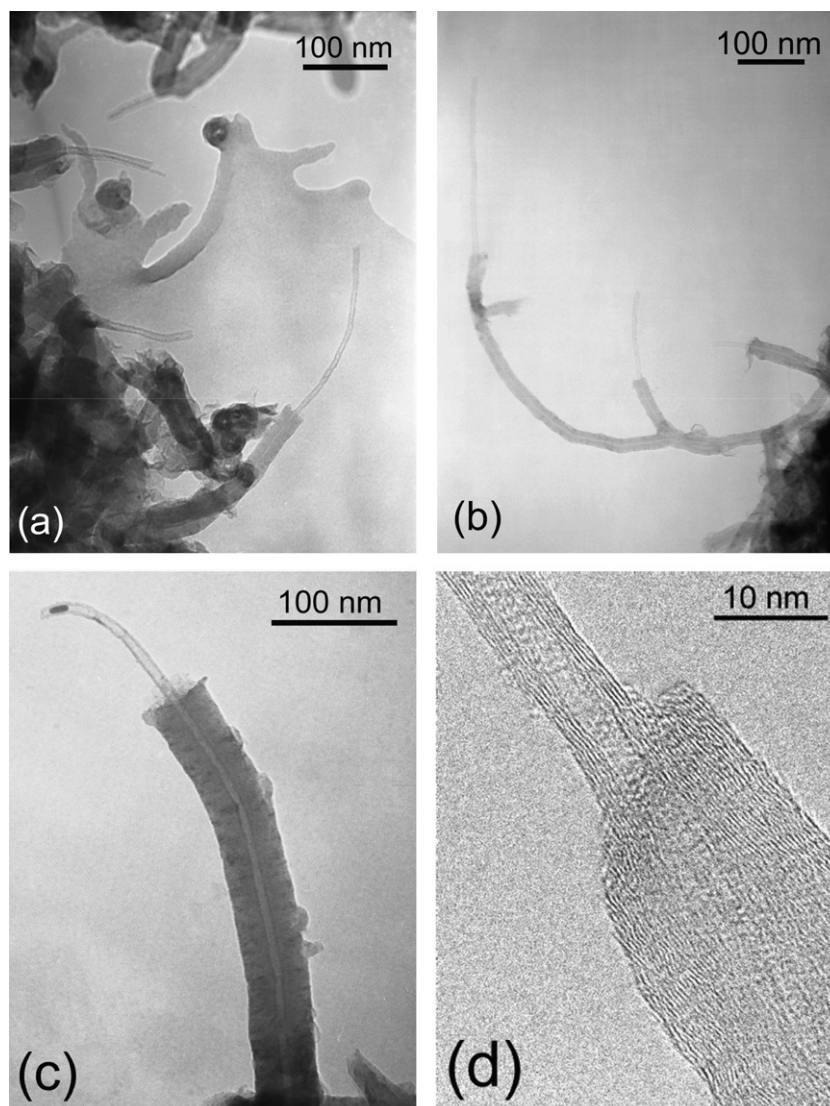


Fig. 4. TEM images (a-c) and HRTEM images (d) of the ‘injector-like’ MWNT/MWNT junctions grown on silica microspheres by two-step CVD with the halfway furnace cooling-down procedure (Scheme 2), furnace temperature was 800 °C at ethyne step.

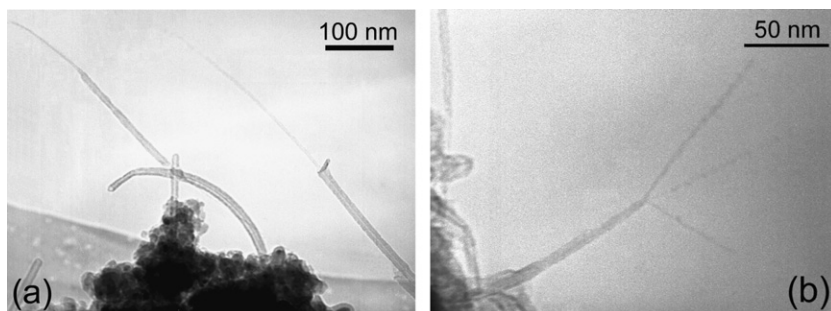


Fig. 5. (a) ‘Injector-like’ CNT junctions grown on porous silica through Scheme 2. (b) Tri-branched CNT junction observed on porous magnesia support through Scheme 2.

SWNTs or DWNTs which jointed with the MWNT tips in the *methane step*.

3.3. Injector-like MWNT’/MWNT nanojunctions obtained by Scheme 2

In the above experiments, the furnace temperature was set to 750 °C in the *ethyne step*. When it was set to 800–850 °C, the products were MWNTs of large diameter and MWNT’/MWNT junctions. The diameters of the thick parts and the thin parts of the MWNT’/MWNT junctions are 25–50 nm and 7–12 nm, respectively (Fig. 4). The higher temperature in *ethyne step* might produce MWNTs with larger inner diameters. And most likely the larger inner diameter led to the formation of MWNT’/MWNT junctions other than SWNT/MWNT ones. Some junctions with remained nanoparticles encapsulated in the tips of thin MWNTs were observed (Fig. 4c). It hints that both thick and thin parts of CNT junctions grew through ‘tip-growth’ mechanism at this condition. Branched junctions (Fig. 4b) were occasionally found in products. Perhaps some iron atoms deposited onto the walls of the formed nanotubes and acted as the catalyst to grow the branched structures by chance [22].

3.4. Nanojunctions obtained with different catalyst support

The injector-like CNT junctions shown in Fig. 5 were obtained with porous silica and magnesia as the catalyst support via Scheme 2. A tri-branched CNT junction structure was observed on the porous magnesia support (Fig. 5b). This trident junction may be formed through the splitting of the catalyst particles at the second CVD step. We found Na-ZSM-5 zeolite can also act as the catalyst support to obtain nanojunctions (see [Supplementary Data](#)). These results show that the two-step CVD process may be a commonly applicable strategy for preparing various CNT junctions.

4. Conclusion

We have developed a simple two-step thermal CVD process to grow CNT junctions. Ethyne and methane were

used as the carbon sources for the first and the second steps, respectively. Cooling down the furnace in the mid-way between the two steps will normally obtain nanojunctions with injector-like morphology. Without the cooling down process, dropper-like nanojunctions will be produced. Relatively low CVD temperature (e.g. 750 °C) at the first step was beneficial to the formation of MWNTs with small inner diameter and led to the formation of nanojunctions between MWNTs and SWNTs or DWNTs. Whereas temperatures higher than 800 °C at the first step resulted in MWNTs with larger inner diameter and led to the formation of MWNT’/MWNT junctions. It seems that the CNT junctions were formed through a tip-growth mechanism. These CNT junctions are expected to be used as scan probe microscope tips, or to build field-emission devices and field-effect devices.

Acknowledgements

This work was supported by the NSF (Project 90406018), MOST (Project 2001CB610501) and MOE of China

Appendix A. Supplementary data

Supplementary data associated with this article can be found, in the online version, at [doi:10.1016/j.cplett.2006.10.025](https://doi.org/10.1016/j.cplett.2006.10.025).

References

- [1] Y. Wu, J. Xiang, C. Yang, W. Lu, C.M. Lieber, *Nature* 430 (2004) 61.
- [2] R.H. Baughman, A.A. Zakhidov, W.A. de Heer, *Science* 297 (2002) 787.
- [3] W.A. de Heer, *MRS Bull.* 29 (2004) 281.
- [4] P. Avouris, *Acc. Chem. Res.* 35 (2002) 1026.
- [5] J. Hu, M. Ouyang, P. Yang, C.M. Lieber, *Nature* 399 (1999) 48.
- [6] Y. Zhang, T. Ichihashi, E. Landree, F. Nihey, S. Iijima, *Science* 285 (1999) 1719.
- [7] J. Luo, L. Zhang, Y. Zhang, J. Zhu, *Adv. Mater.* 14 (2002) 1413.
- [8] J. Luo, Z. Huang, Y. Zhao, L. Zhang, J. Zhu, *Adv. Mater.* 16 (2004) 512.
- [9] S. Iijima, T. Ichihashi, Y. Ando, *Nature* 356 (1992) 776.
- [10] S. Iijima, *Mater. Sci. Eng. B* 19 (1993) 172.
- [11] B.I. Dunlap, *Phys. Rev. B* 49 (1994) 5643.

- [12] L. Chico, V.H. Crespi, L.X. Benedict, S.G. Louie, M.L. Cohen, *Phys. Rev. Lett.* 76 (1996) 971.
- [13] Z. Yao, H.W.C. Postma, L. Balents, C. Dekker, *Nature* 402 (1999) 273.
- [14] M. Ouyang, J. Huang, C. Cheung, C.M. Lieber, *Science* 291 (2001) 97.
- [15] S.K. Doorn, M.J. O'Connell, L. Zheng, Y. Zhu, S. Huang, J. Liu, *Phys. Rev. Lett.* 94 (2005) (Art. No. 016802).
- [16] L. Liu, S. Fan, *J. Am. Chem. Soc.* 123 (2001) 11502.
- [17] J. Suh, J. Lee, H. Kim, *Synth. Met.* 123 (2001) 381.
- [18] Y. Li, S. Xie, W. Zhou, Y. Bando, *Carbon* 41 (2003) 380.
- [19] A.M. Cassell, J. Li, R. Stevens, J.E. Koehne, L. Delzeit, H.T. Ng, *Appl. Phys. Lett.* 85 (2004) 2364.
- [20] P. Hu, K. Xiao, Y. Liu, G. Yu, X. Wang, L. Fu, *Appl. Phys. Lett.* 84 (2004) 4932.
- [21] J. Guo, C. Zhi, X. Bai, E. Wang, *Appl. Phys. Lett.* 80 (2002) 124.
- [22] N. Gothard, C. Daraio, J. Gaillard, R. Zidan, S. Jin, A.M. Rao, *Nano Letter* 4 (2004) 213.
- [23] Y. Li, J. Liu, Y. Wang, Z.L. Wang, *Chem. Mater.* 13 (2001) 1008.